

Single Quantum Dot-Micelles Coated with Silica Shell as Potentially Non-Cytotoxic Fluorescent Cell Tracers

Zhivko Zhelev, Hideki Ohba, and Rumiana Bakalova*

On-Site Sensing and Diagnosis Research Laboratory, National Institute of Advanced Industrial Science and Technology, AIST-Kyushu, 807-1 Shuku-machi, Tosu 841-0052, Japan

Received February 17, 2006; E-mail: r.bakalova-zheleva@aist.go.jp

In the earlier studies describing a development of hybrid materials on the basis of quantum dots (QDs) incorporated into silica spheres, the synthesis of QDs has been performed in water phase or in water-to-oil microemulsion. This methodology does not allow the synthesis of high-quality QDs with high quantum yield (QY) and sharp photoluminescence (PL) spectra. In most cases, there is accumulation of QD aggregates into the silica spheres, and the size of QD-doped silica particles exceeds 50 nm.

The synthesis of ligand-capped QDs by Murray's route¹ and their subsequent transfer into silica particles seems to be the most correct approach, because it proceeds from QDs with higher quality. Currently, two groups have demonstrated a synthesis of silica-coated QDs (synthesized by Murray's route) consisting of a single nanocrystal into one silica sphere.² The obtained nanoparticles are uniform, with relatively narrow size distribution; however, they are characterized with comparatively low QY (up to 18%), presumably as a result of the preliminary exchange of the coordinating ligands before addition of silica precursors. Moreover, the exchange of surface-coordinating ligands does not allow an incorporation of other hydrophobic substances in these nanoparticles, which can stabilize the spectral characteristics of the overcoated QDs.

Silica-coating of ligand-capped CdSe QDs without preliminary exchange of the coordinating ligands and using a surfactant-assisted microemulsion technique was recently reported.³ However, this methodology results in incorporation of many or at least several QDs into one silica sphere. Apparently, with the use of microemulsion system it is not possible to obtain a large population of single QDs into the silica particles. The reported size of these silica-coated QDs is ~30–150 nm in diameter. Their QY is ~6–8 times lower than the QY of QDs in organic solvents.

In this study, we describe a synthesis of silica-shelled single-QD micelles without exchange of the surface-coordinating ligands (e.g., TOPO, HDA, or ODA). The obtained product consists up to 92% of a single nanocrystal (CdSe, CdSe/ZnS, or CdSe/ZnSe/ZnS) into one silica sphere. The silica-shelled single QD micelles possess a high QY in aqueous solution (only 30–50% lower than the QY of the initial QDs in chloroform), a comparatively small size (up to 18 nm in diameter), a sharp size distribution (~12%), PL and absorbance spectra have the same profile as the corresponding spectra of QDs in organic solvent (e.g., fwhm of PL spectra ~30 nm), an absence of aggregation, and a high transparency. They manifest a possibility for intracellular delivery without application of any other transfection technique. The silica-shelled single QD micelles are amino functionalized and ready for bioconjugation. The presence of a hydrophobic layer between the QD and silica-shell ensures an incorporation of other hydrophobic molecules with interesting properties (e.g., photosensitizers, other dyes, membrane stabilizers, lipid-soluble antioxidants or prooxidants, etc.) in the close proximity of the nanocrystal. Thus, it is possible to combine the characteristics of hybrid material with the priority of small size.

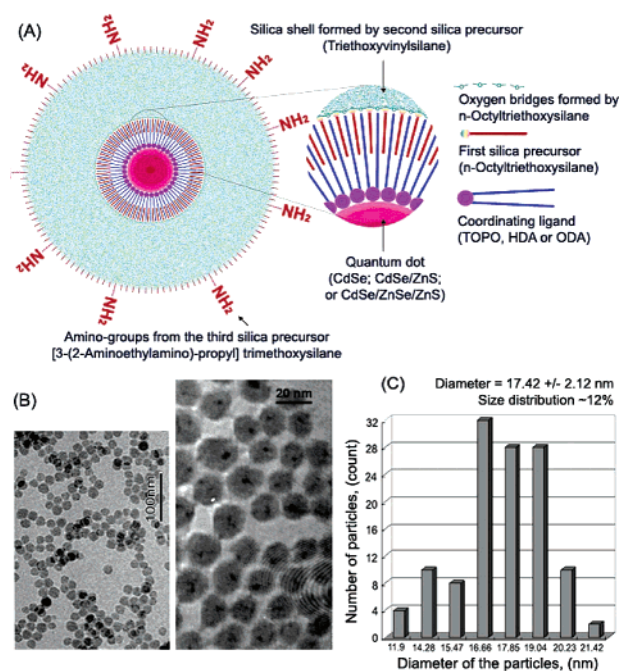


Figure 1. (A) Model structure of a silica-shelled single QD micelle. (B) Representative TEM images of a large population of silica-shelled single CdSe/ZnS QD micelles (ready for bioconjugation). (C) Size-histogram of this population. Inside the silica spheres there are dark spots, indicating single QD nanocrystals.

The development of our silica-shelled QD micelles is based on three recent studies about the incorporation of inorganic QDs into surfactant/lipid micelles⁴ and about the synthesis of QD-doped silica micelles.⁵ In our study, the silica-shelled single QD micelles were synthesized in four steps, using three different silica precursors consecutively (details are described in Supporting Information). The first two silica precursors stabilize the micelle and ensure comparatively high QY of the obtained silica-shelled single QDs in aqueous solutions. The third silica precursor functionalizes the surface and makes it ready for bioconjugation.

The model structure of the product is presented in Figure 1A. The micelle part of the product consists of: (1) a single inorganic nanocrystal (CdSe, CdSe/ZnS, or CdSe/ZnSe/ZnS QD) capped with hydrophobic coordinating ligands (e.g., TOPO, HDA, or ODA); (2) a hydrophobic chain of the first silica precursor (*n*-octyltriethoxysilane, OTS); (3) additional molecules with hydrophobic properties could be also incorporated into the hydrophobic environment of the micelle to stabilize it and to increase the QY of the product.

A silica shell, formed by the second silica precursor (triethoxyvinylsilane, TEVS), covers the micelle. Finally, the surface of the silica sphere is amino functionalized by the third silica precursor

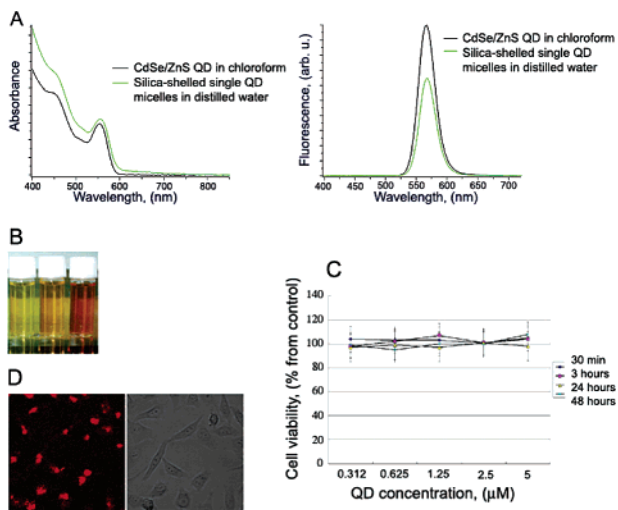


Figure 2. (A) Representative absorbance and fluorescence spectra of CdSe/ZnS QD in chloroform and silica-shelled single CdSe/ZnS QD micelles in distilled water. (B) Images of silica-shelled single CdSe/ZnS QD micelles in three colors. (C) Cytotoxicity of silica-shelled single CdSe/ZnS QD micelles in viable HeLa cells. (D) Intracellular delivery (fluorescence confocal microscopic image) of silica-shelled single CdSe/ZnS QD micelles in viable HeLa cells.

[3-(2-aminoethylamino)-propyl]-trimethoxysilane. Thus, the final product is ready for bioconjugation. The ζ -potential titration provided a proof of cationic surface modification. At acidic pH (3.0) the particles had a surface potential of +28 mV, which decreased to -31 mV at pH 10. At physiological pH (7.4), the ζ -potential was +6.5 mV.

The TEM images demonstrate that the silica-shelled single QD micelles are quite uniform in size (Figure 1B) with diameter 17.72 ± 2.12 nm and size-distribution $\sim 12\%$ (Figure 1C). The population consists in $\sim 92\%$ of single QD micelle into one silica sphere, in $\sim 6\%$ of two QD micelles into one silica sphere, and in $\sim 2\%$ of empty silica spheres (without QDs).

The incorporation of single QD into one silica sphere excludes the possibility for fluorescence self-quenching as a result of concentration of many nanocrystals into the small volume of one silica sphere. Moreover, the micelle structure additionally preserves the surface of the nanocrystal and increases the QY of the final product in aqueous solutions. The QY of our silica-shelled single QD micelles depended on (i) the type of QD; (ii) its initial QY in chloroform; and (iii) the presence or absence of other hydrophobic molecules into the micelle part of the nanoparticle (e.g., cholesterol, hexane, or toluene) (Table 1S, Figure 2S). In the case of silica-shelled CdSe/ZnS or CdSe/ZnSe/ZnS micelles, the QY was approximately 30–50% lower than the QY of the initial QDs in chloroform. It was stable in 20 mM Tris-HCl buffer (pH 6.5–7.3) and in distilled water. The QY of amino-functionalized nanoparticles decreased slightly in high-salt phosphate or carbonate buffers. However, the exchange of amino groups with carboxyl groups on the surface preserved the QY in high-salt phosphate and carbonate buffers at physiological pH. The incorporation of cholesterol, toluene, or hexane into the micelle part increased the QY. The spectral characteristics of CdSe/ZnS QDs before and after silica-shelling are presented in Figure 2A. The size-tunable absorbance and emission spectra of the silica-shelled QD micelles have the same profile as the respective spectra of QD in chloroform. The absorbance spectrum is slightly raised after silica-shelling, probably as a result of light scattering from particles with size > 12 nm. The

amplitude of the fluorescence spectrum decreases $\sim 30\%$ after silica-shelling; however, the fwhm does not change (it is ~ 30 nm.). The samples are also characterized with high transparency (Figure 2B). The high structural homogeneity of the obtained nanoparticles (composed up to 92% of single QD into one silica sphere) and the preservation of the absorbance spectrum profile allow a definition of their exact concentration in aqueous solution, which is obligatory in life science experiments, especially in experiments on viable cells and animals. The concentration of silica-shelled QD micelles is closely related to the concentration of QD in moles, calculated by the method of Yu et al.⁶ In the case of silica particles containing nondefined amount of QDs, it is rather complicated to define the exact concentration of the nanoparticles in aqueous solutions, which is a serious restriction for quantitative bioanalyses.

In the absence of light exposure, the silica-shelled QDs were noncytotoxic up to $5 \mu\text{M}$ QD concentration and 48 h incubation with cultured cell lines [HeLa, Jurkat, and K-562 (Figure 2C, Table 2S)], which makes them appropriate for long-term treatment of cells and even animals (PEG-conjugated silica-shelled QDs showed a comparatively long-term stability in microcirculation: half-life ~ 7 h, detected in mice; data are not shown). However, under UV irradiation, the nanoparticles manifested a slight cytotoxicity. Since the release of free Cd from the silica particles is not likely under the selected experimental conditions,^{7a} the cytotoxic effect can be explained with the photosensitizing properties of the silica-shelled QD micelles and the possibility for UV-induced generation of reactive oxygen species and free radicals.⁷ Obviously, the silica shell did not suppress the access of small-sized molecules (e.g., oxygen) and ions to the nanocrystal surface.

The silica-shelled QD micelles possess a comparatively good intracellular delivery (without application of any other transfection technique) (Figure 2D), probably because of the large positive charge on their surface and comparatively small size. Thus, the nanoparticles can be highly concentrated into the cells (cytoplasm and/or nucleus), which will increase the signal-to-noise ratio and will improve the quality of the images. The comparatively easy penetration of these nanoparticles into viable cells and the possibility for conjugation with different chemical substances makes them also appropriate for drug delivery.

Acknowledgment. The technical assistance of Dr. Yusuke Imai in TEM-imaging is gratefully acknowledged.

Supporting Information Available: Experimental procedures. This material is available free of charge via the Internet at <http://pubs.acs.org>.

References

- (1) Murray, C. B.; Norris, D. J.; Bawendi, M. G. *J. Am. Chem. Soc.* **1993**, *115*, 8706–8715.
- (2) (a) Gerion, D.; Pinaud, F.; Williams, S. C.; Parak, W. J.; Zanchet, D.; Weiss, S.; Alivisatos, A. P. *J. Phys. Chem. B* **2001**, *105*, 8861–8871. (b) Nann, T.; Mulvaney, P. *Angew. Chem., Int. Ed.* **2004**, *43*, 5393–5396.
- (3) (a) Kim, J.; Lee, J. E.; Lee, J.; Yu, J. H.; Kim, B. C.; An, K.; Hwang, Y.; Shin, C.-H.; Park, J.-G.; Kim, J.; Hyeon, T. *J. Am. Chem. Soc.* **2006**, *128*, 688–689. (b) Yi, D. K.; Selvan, S. T.; Lee, S. S.; Papaefthymiou, G. C.; Kundaliya, D.; Ying, J. Y. *J. Am. Chem. Soc.* **2005**, *127*, 4990–4991.
- (4) Fan, H.; Leve, E. W.; Scullin, C.; Gabaldon, J.; Tallant, D.; Bunge, T.; Wilson, Brinker, C. J. *Nano Lett.* **2005**, *5*, 645–648.
- (5) (a) Chen, Y.; Rosenzweig, Z. *Nano Lett.* **2002**, *2*, 1299–1302. (b) Fan, H.; Chen, Z.; Brinker, C. J.; Clawson, J.; Alam, T. *J. Am. Chem. Soc.* **2005**, *127*, 13746–13747.
- (6) Yu, W. W.; Qu, L.; Guo, W.; Peng, X. *Chem. Mater.* **2003**, *15*, 2854–2860.
- (7) (a) Bakalova, R.; Ohba, H.; Zhelev, Z.; Nagase, T.; Jose, R.; Ishikawa, M.; Baba, Y. *Nano Lett.* **2004**, *4*, 1567–1573. (b) Tsay, J. M.; Michalek, X. *Chem. Biol.* **2005**, *12*, 1159–1160.

JA061137D